

# Direct Comparison of Electrochemical and Spectrochemical Kinetics for Catalytic Oxygen Reduction

Derek J. Wasylenko, Carlos Rodríguez, Michael L. Pegis, and James M. Mayer<sup>\*,†</sup>

Department of Chemistry, University of Washington, Seattle, Washington 98195-1700, United States

**S** Supporting Information

**ABSTRACT:** We describe here a direct comparison of electrochemical and spectrochemical experiments to determine rates and selectivity of oxygen reduction catalyzed by iron 5,10,15,20-*meso*-tetraphenylporphyrin chloride. Good agreement was found between the two methods, suggesting the same mechanism is occurring under both conditions, with the same third-order rate law, similar selectivity, and the derived rate constants agreeing within a factor of at most 4, with  $k_{\text{cat}} \cong 2 \times 10^6 \text{ M}^{-2} \text{ s}^{-1}$ . This Communication provides a rare example of a redox catalytic process characterized by two common but very different methods.

Many next-generation energy technologies are based on the catalytic interconversion of energy stored in chemical bonds with electrical energy. Electrochemical techniques are ideally suited in this endeavor and have been well developed for heterogeneous electrocatalysts.<sup>1</sup> Electrochemical techniques are also being increasingly used to study homogeneous catalytic systems.<sup>2</sup> Such studies are complicated by the subtle interplay between parameters affecting the relative concentrations of catalyst, substrate, and intermediary species in the reaction–diffusion layer. We demonstrate here the congruence of the new electrochemical “foot-of-the-wave” (FOW) analysis<sup>3</sup> with more traditional spectrochemical kinetic analysis for a catalytic oxygen reduction reaction (ORR; eq 1).



The ORR is a prototypical electrocatalytic reaction and a key half-reaction in many fuel cells and next-generation battery technologies.<sup>4</sup> The goals for new ORR electrocatalysts are high activity at low overpotentials, low cost, long lifetime, and high selectivity for the  $4\text{e}^-/4\text{H}^+$  reduction to  $\text{H}_2\text{O}$  over the  $2\text{e}^-/2\text{H}^+$  production of  $\text{H}_2\text{O}_2$ .<sup>4,5</sup> Iron porphyrin complexes such as iron 5,10,15,20-*meso*-tetraphenylporphyrin chloride ( $[\text{Fe}^{\text{III}}(\text{TPP})\text{Cl}]$ ) were among the earliest targets for molecular complexes to catalyze the ORR.<sup>6</sup> This was due to their similarity to the heme active sites present in many  $\text{O}_2$ -binding proteins and  $\text{O}_2$ -reducing enzymes. Decades of research have produced highly elegant and biomimetic structures.<sup>5,7,8</sup> The present study provides some of the first kinetic and mechanistic details for understanding catalysis of the ORR by simpler iron porphyrin complexes. It is therefore a benchmark for more complex catalysts, including our recent catalysts that include proton

relays into iron porphyrin ORR catalysts,<sup>9</sup> for which  $[\text{Fe}^{\text{III}}(\text{TPP})\text{Cl}]$  represents the archetypical system.

We show here that the kinetic information from FOW analysis of voltammetric data is in good agreement with that from more standard spectrochemical techniques. This parallel electrochemical and spectrochemical study not only validates the electrochemical approach but also illustrates how to use both techniques in parallel for studying complex multi-electron, multi-proton redox catalytic reactions.

**1. Electrochemical Kinetics.** Figure 1 displays a representative cyclic voltammogram (CV) of  $[\text{Fe}^{\text{III}}(\text{TPP})\text{Cl}]$

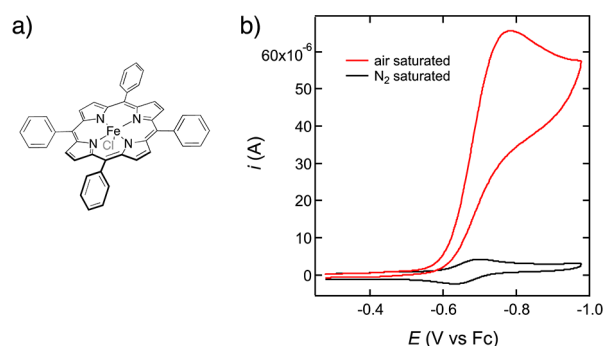


**Figure 1.** (a) Structure of the catalyst  $[\text{Fe}^{\text{III}}(\text{TPP})\text{Cl}]$ . (b) CVs of 0.45 mM  $[\text{Fe}^{\text{III}}(\text{TPP})\text{Cl}]$  in DMF with 0.1 M  $[\text{Bu}_4\text{N}][\text{PF}_6]$ , 6 mM LiCl, and 30 mM  $\text{HClO}_4$  under 1 atm air (red) or 1 atm  $\text{N}_2$  (black) with a 3 mm diameter glassy carbon electrode at  $100 \text{ mV s}^{-1}$ .

in *N,N'*-dimethylformamide (DMF) with an excess of strong acid ( $\text{HClO}_4$ ) in the presence and absence of  $\text{O}_2$ . The much higher currents in the presence of  $\text{O}_2$  indicates substantial catalytic activity that occurs at the onset of the Fe(III/II) redox couple ( $E_{\text{Fe(III/II)}}$ ). All experiments reported herein were performed in the presence of LiCl (10–20 equiv) in order to minimize issues from  $\text{Cl}^-$  ligand exchange<sup>10</sup> that complicate kinetic analysis (see Supporting Information, Figures S2–S4). Catalytic rate constants  $k_{\text{obs}}$  were determined as a function of the concentrations of  $\text{HClO}_4$  and  $\text{O}_2$ . Briefly, FOW analysis derives  $k_{\text{obs}}$  from the ratio of catalytic currents ( $i_{\text{cat}}$ ) to peak current in the absence of  $\text{O}_2$  ( $i_p$ ) as a function of the applied potential,  $(1 + \exp[(F/RT)(E - E_{\text{Fe(III/II)})])^{-1}$ .<sup>3a</sup> A linear relationship is predicted in regions of “well-behaved” electrocatalysis (eq 2).

Received: June 11, 2014

Published: August 19, 2014

$$\frac{i_{\text{cat}}}{i_{\text{p}}} = \frac{2.24(n_{\text{cat}})^{\sigma} \sqrt{\frac{RT}{F\nu}} k_{\text{obs}}}{1 + \exp\left[\frac{F}{RT}(E - E_{\text{Fe(III/II)}})\right]} \quad (2)$$

“Well-behaved” in this context means that (i) heterogeneous electron transfer steps are sufficiently rapid such that catalysis is limited by homogeneous (chemical) steps; (ii) catalysis is not limited by diffusion of substrates (i.e.,  $\text{O}_2$ ,  $\text{H}^+$ ) to the reaction layer; and (iii) no significant deactivation of the catalyst is occurring.  $k_{\text{obs}}$  values can then be obtained from the slope of the FOW plot,  $2.24(n_{\text{cat}})^{\sigma}[(RT/F\nu)k_{\text{obs}}]^{1/2}$ , where  $\nu$  is the scan rate in  $\text{V s}^{-1}$ ,  $n_{\text{cat}}$  is the number of electrons transferred in the catalytic reaction, and  $\sigma$  is a stoichiometric factor depending on the mechanism ( $0.5 \leq \sigma \leq 1$ , taken as  $\sim 1$  here, *vide infra*).<sup>11</sup> The major advantage of FOW analysis is that catalysis is slow in the “foot” region, minimizing the complications mentioned above. With the more common electrochemical kinetic equations, achieving the required “kinetic conditions” can be challenging, especially given the low  $[\text{O}_2]$ .<sup>9</sup> However, FOW analysis is highly sensitive to the apparent potential of the active redox couple. In this system, obtaining accurate FOW rate constants required accounting for the shift in  $E_{\text{Fe(III/II)}}$  with increasing  $[\text{HClO}_4]$  (Figure S3).

Cathodic CV segments of  $[\text{Fe}^{\text{III}}(\text{TPP})\text{Cl}]$  as a function of  $\text{HClO}_4$  in DMF under 1 atm  $\text{O}_2$  are shown in Figure 2a. Subsequent FOW analysis (Figure 2b) determined the  $k_{\text{obs}}$  values (Figure 2c). (See Figures S5–S7 for full CVs and descriptions of the method.) Under 1 atm  $\text{O}_2$  ( $[\text{O}_2] = 3.1 \text{ mM}$ ),<sup>12</sup>  $k_{\text{obs}}$  varies linearly with  $[\text{HClO}_4]$ , yielding an apparent second-order rate constant,  $k_{\text{H}^+} = (3.7 \pm 0.2) \times 10^3 \text{ M}^{-1} \text{ s}^{-1}$ . Furthermore, a plot of  $\log(k_{\text{obs}})$  vs  $\log[\text{HClO}_4]$  has a slope of 0.95 (Figure S8), indicating a first-order dependence on  $\text{HClO}_4$ . The catalysis, and the  $E_{\text{Fe(III/II)}}$  in the absence of  $\text{O}_2$ , are not significantly affected by the presence of  $\text{H}_2\text{O}$  (Figures S4 and S9).

A similar series of experiments was conducted at constant  $[\text{HClO}_4]$  with three different  $[\text{O}_2]$  (0.65, 1.6, and 3.1 mM, Figures S10 and S11). The FOW analysis is particularly valuable here because in the foot-of-the-wave region there is no depletion of the low-concentration  $\text{O}_2$  substrate near the electrode.  $k_{\text{obs}}$  varies linearly with  $[\text{O}_2]$ , yielding an apparent  $k_{\text{O}_2} = (2.0 \pm 0.3) \times 10^4 \text{ M}^{-1} \text{ s}^{-1}$  (with 20 mM  $\text{HClO}_4$ ). Finally, the catalytic currents vary linearly with  $[\text{Fe}^{\text{III}}(\text{TPP})\text{Cl}]$ , indicating a

first-order dependence (Figure S12). Altogether, these results indicate a rate law of the form

$$\begin{aligned} \text{rate} &= k_{\text{obs}}[\text{Fe}^{\text{III}}(\text{TPP})\text{Cl}] \\ k_{\text{obs}} &= k_{\text{cat}}[\text{O}_2][\text{HClO}_4] \\ k_{\text{cat}} &= k_{\text{O}_2}/[\text{HClO}_4] = k_{\text{H}^+}/[\text{O}_2] \end{aligned} \quad (3)$$

The third-order overall rate constant,  $k_{\text{cat}}$ , is determined from  $k_{\text{O}_2}$  to be  $(1.0 \pm 0.2) \times 10^6 \text{ M}^{-2} \text{ s}^{-1}$  and from  $k_{\text{H}^+}$  to be  $(1.2 \pm 0.1) \times 10^6 \text{ M}^{-2} \text{ s}^{-1}$ . The agreement between these values confirms the third-order kinetics with the weighted average,  $k_{\text{cat}} = (1.1 \pm 0.1) \times 10^6 \text{ M}^{-2} \text{ s}^{-1}$ .

**2. Spectrochemical Kinetics.** The homogeneous catalytic reaction was examined using stopped-flow techniques by mixing, in a typical experiment, a DMF solution of  $\text{O}_2$  (0.65 mM),  $\text{HClO}_4$  (42 mM),  $[\text{Fe}^{\text{III}}(\text{TPP})\text{Cl}]$  (60  $\mu\text{M}$ ), and  $\text{LiCl}$  (1.2 mM) with an equal volume of an anaerobic DMF solution with excess of the reductant decamethylferrocene ( $\text{Fc}^*$ , 8.0 mM; all concentrations decreased by half upon mixing). Both solutions were kept at constant ionic strength using  $[\text{Bu}_4\text{N}][\text{PF}_6]$  (0.1 M). In these typical reaction conditions, the electrolyte and  $\text{LiCl}$  were added to mimic the electrochemical conditions.  $\text{Fc}^*$  was chosen as a reasonably strong reductant ( $E_{1/2} = -0.48 \text{ V}$  vs  $\text{Fc}$ ; Figure S13).  $\text{Fc}^*$  slowly reduces  $\text{O}_2$  in the presence of strong acids,<sup>13</sup> but no substantial oxidation of  $\text{Fc}^*$  occurs over the time scale of our experiments (Figure S14).

Reaction progress was monitored by the appearance of  $\text{Fc}^{*+}$  by UV–vis spectroscopy (Figure 3a). With  $[\text{Fe}^{\text{III}}(\text{TPP})\text{Cl}] \ll [\text{O}_2] < [\text{Fc}^*] < [\text{HClO}_4]$ , the rate of formation of  $\text{Fc}^{*+}$  obeyed pseudo-first-order kinetics typically over at least three half-lives. Pseudo-first-order rate constants increased linearly with increasing concentrations of  $[\text{HClO}_4]$  or  $[\text{Fe}^{\text{III}}(\text{TPP})\text{Cl}]$ , while no dependence was observed on  $[\text{Fc}^*]$  (Figure 3b–d). These results indicate a rate law for the overall catalytic  $\text{O}_2$  reduction reaction shown in eq 4, in which  $n_{\text{cat}}$  is the number of  $\text{Fc}^{*+}$  per  $\text{O}_2$  consumed (3.7, *vide infra*).

$$\begin{aligned} \text{rate} &= n_{\text{cat}} d[\text{Fc}^{*+}]/dt = k_{\text{obs}}[\text{O}_2] \\ k_{\text{obs}} &= k_{\text{cat}}[\text{Fe}(\text{TPP})\text{Cl}][\text{HClO}_4] \\ k_{\text{cat}} &= k_{\text{Fe}}/[\text{HClO}_4] = k_{\text{H}^+}/[\text{Fe}(\text{TPP})\text{Cl}] \end{aligned} \quad (4)$$

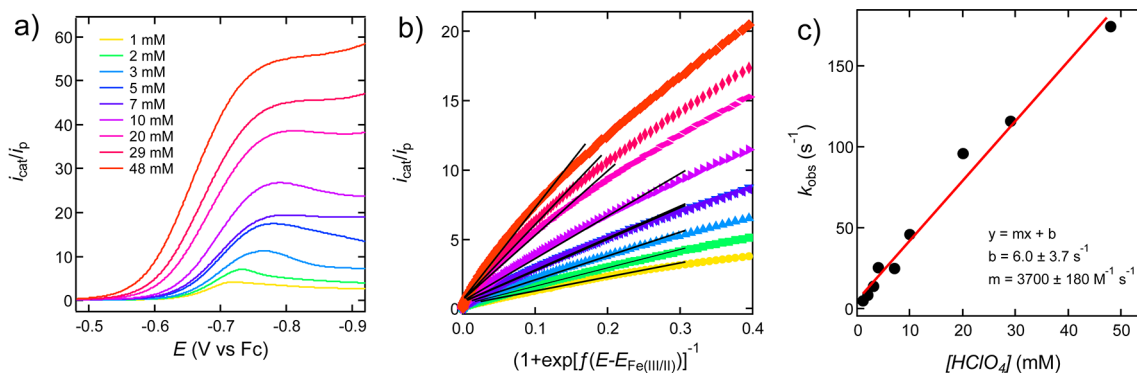


**Figure 2.** (a) Cathodic sweeps of CVs of 0.40 mM  $[\text{Fe}^{\text{III}}(\text{TPP})\text{Cl}]$  in DMF with 0.1 M  $[\text{Bu}_4\text{N}][\text{PF}_6]$ , 6 mM  $\text{LiCl}$ , and varying  $[\text{HClO}_4]$  under 1 atm  $\text{O}_2$  with a 3 mm diameter glassy carbon electrode at  $100 \text{ mV s}^{-1}$ . (b) Corresponding FOW plots with black lines indicating fitting regions,  $f = F/RT$ . (c)  $k_{\text{obs}}$  derived from FOW analysis as a function of  $[\text{HClO}_4]$ .

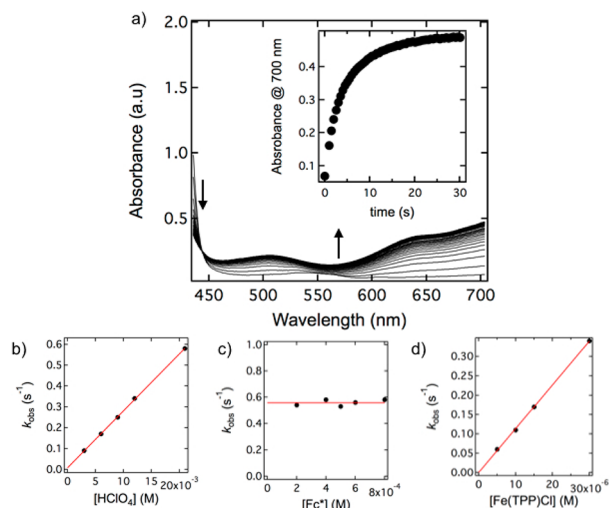


**Figure 3.** (a) UV-vis spectral changes during the reduction of  $\text{O}_2$  (0.33 mM) by  $\text{Fc}^*$  (4 mM) and  $\text{HClO}_4$  (10 mM) catalyzed by  $[\text{Fe}^{\text{III}}(\text{TPP})\text{Cl}]$  (15  $\mu\text{M}$ ) +  $\text{LiCl}$  (0.3 mM). Inset: time profile for the absorbance at 700 nm associated with  $\text{Fc}^{*\text{+}}$  formation. Below: Plots of (b)  $k_{\text{obs}}$  vs  $[\text{HClO}_4]$  with  $[\text{Fe}^{\text{III}}(\text{TPP})\text{Cl}] = 30 \mu\text{M}$ ; (c)  $k_{\text{obs}}$  vs  $[\text{Fc}^*]$  with  $[\text{HClO}_4] = 21 \text{ mM}$  and  $[\text{Fe}^{\text{III}}(\text{TPP})\text{Cl}] = 30 \mu\text{M}$ ; and (d)  $k_{\text{obs}}$  vs  $[\text{Fe}^{\text{III}}(\text{TPP})\text{Cl}]$  with  $[\text{HClO}_4] = 12.5 \text{ mM}$ ,  $[\text{O}_2] = 0.33 \text{ mM}$ , and  $[\text{Fc}^*] = 4 \text{ mM}$ .

In the spectrochemical case,  $k_{\text{H}^+} = 101 \pm 2 \text{ M}^{-1} \text{ s}^{-1}$  (at 30  $\mu\text{M}$   $\text{Fe}$ ; Figure 3b) and  $k_{\text{Fe}} = (4.1 \pm 0.7) \times 10^4 \text{ M}^{-1} \text{ s}^{-1}$  (at 12.5 mM  $\text{HClO}_4$ ; Figure 3d). The resulting third-order overall rate constants are in excellent agreement,  $k_{\text{cat}} = (3.4 \pm 0.4) \times 10^6 \text{ M}^{-2} \text{ s}^{-1}$  from  $k_{\text{H}^+}$  and  $(3.4 \pm 0.7) \times 10^6 \text{ M}^{-2} \text{ s}^{-1}$  from  $k_{\text{Fe}}$  for a weighted average value of  $k_{\text{cat}} = (3.4 \pm 0.5) \times 10^6 \text{ M}^{-2} \text{ s}^{-1}$ .

**3. Catalytic Selectivity.** The selectivity of  $\text{O}_2$  reduction,  $4\text{e}^-/4\text{H}^+$  to  $\text{H}_2\text{O}$  or  $2\text{e}^-/2\text{H}^+$  to  $\text{H}_2\text{O}_2$ , has been addressed electrochemically by rotating ring-disc voltammetry (RRDV). RRDV is usually used for thin films of catalytic material on the electrode surface; however, it can provide estimates of selectivity for homogeneous electrocatalysts under certain conditions (described in detail in the SI and Figure S15).<sup>14</sup> Figure 4 displays RRDV of  $[\text{Fe}^{\text{III}}(\text{TPP})\text{Cl}]$  collected under conditions similar to the electrochemical kinetics described above. The ratio of ring current to disc current then provides an estimate of the amount of  $\text{H}_2\text{O}_2$  produced at 10–20%.

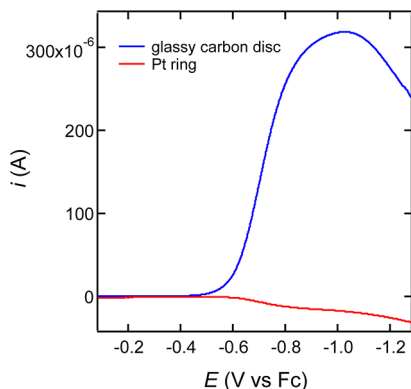


**Figure 4.** Rotating ring-disc voltammograms of 0.5 mM  $[\text{Fe}^{\text{III}}(\text{TPP})\text{Cl}]$  in DMF with 0.1 M  $[\text{Bu}_4\text{N}][\text{PF}_6]$ , 5 mM  $\text{LiCl}$ , 50 mM  $\text{HClO}_4$  under 1 atm  $\text{O}_2$  at  $20 \text{ mV s}^{-1}$  and rotation rate 400 rpm; ring potential = +0.55 V vs Fc.

In the spectroscopic experiments, the stoichiometry of the reaction under conditions of limiting  $\text{O}_2$  and excess  $\text{Fc}^*$  and  $\text{HClO}_4$  is indicated by the amount of  $\text{Fc}^{*\text{+}}$  produced. A solution containing 0.33 mM  $\text{O}_2$  gave 1.2 mM  $\text{Fc}^{*\text{+}}$  when the reaction was complete. This is  $\sim 90\%$  of the total possible formation of  $\text{Fc}^{*\text{+}}$ , if all of the  $\text{O}_2$  had been reduced to water. Iodometric titrations immediately after reaction confirmed that  $10 \pm 3\%$   $\text{H}_2\text{O}_2$  was formed (Figure S16).<sup>15</sup> This value is in reasonable agreement with the RRDV studies (both give  $n_{\text{cat}} \approx 3.7\text{e}^-/\text{O}_2$ ). Under these conditions, the disproportionation of  $\text{H}_2\text{O}_2$  by  $[\text{Fe}^{\text{III}}(\text{TPP})\text{Cl}]$  or a reduced form of  $[\text{Fe}^{\text{III}}(\text{TPP})\text{Cl}]$  are kinetically slow (Figures S17 and S18, respectively).

**4. Comparison of Electrochemical and Spectrochemical Results.** Kinetic investigations with the two techniques each give the same third-order rate law. The selectivities determined by electrochemical RRDV and iodometric titrations agree reasonably well. Comparison of the third-order rate constants measured by the two techniques is complicated by the uncertainty in the stoichiometric exponent  $\sigma$  in eq 2. If the catalyst is always reduced by the electrode,  $\sigma = 1$ , then the derived values differ by a factor of 4. If there are homogeneous quasi-disproportionation steps  $\sigma$  approaches 0.5, and the values agree within a factor of 2.<sup>11</sup> Collectively these results indicate that the catalytic processes are similar in the vicinity of the electrode and in the bulk solution. The rate law is consistent with a mechanism whereby a rapidly generated  $\text{Fe}(\text{II})$  species undergoes reversible  $\text{O}_2$  binding followed by rate-limiting protonation, as will be discussed in a future publication.

A direct comparison of the two kinetic methods is possible here because the spectrochemical kinetics are independent of the concentration of reductant ( $\text{Fc}^*$ ). This implies that all reduction steps prior to the rate-limiting step rapidly proceed to completion. The conditions of the spectrochemical kinetic experiments are therefore analogous to Savéant's electrochemical "kinetic regime", where the current is independent of the applied potential.<sup>2a</sup> As a result, the same homogeneous chemical steps that are intrinsic to the catalyst limit the catalytic reaction in both experimental methods, consequently leading to congruent outcomes for both  $k_{\text{cat}}$  and catalytic selectivity.

In summary, we have examined oxygen reduction catalyzed by  $[\text{Fe}^{\text{III}}(\text{TPP})\text{Cl}]$  using the recently introduced electrochemical FOW analysis and compared the results obtained from traditional spectrochemical methods. Under these conditions, both methodologies derive kinetic information about the intrinsic chemical capability of  $[\text{Fe}^{\text{III}}(\text{TPP})\text{Cl}]$  to catalyze the ORR, independent of the electron transfer steps. The same rate law, similar third-order catalytic rate constants, and very similar selectivity are found with the two methods. The congruence of the two techniques is an important finding for the redox catalysis community. Given that research related to catalytic energy conversion is at the forefront of the chemical sciences at present, these findings provide a timely validation for the rapidly growing area of molecular electrocatalytic studies. Future reports will explore the mechanism of the ORR catalyzed by a variety of iron porphyrin complexes, using these complementary techniques.

## ■ ASSOCIATED CONTENT

### Supporting Information

Electrochemical and spectrochemical methods and additional experiments. This material is available free of charge via the Internet at <http://pubs.acs.org>.

## AUTHOR INFORMATION

### Corresponding Author

james.mayer@yale.edu

### Present Address

<sup>†</sup>J.M.M.: Department of Chemistry, Yale University, New Haven, CT 06520-8107

### Notes

The authors declare no competing financial interest.

## ACKNOWLEDGMENTS

This work was supported as part of the Center for Molecular Electrocatalysis, an Energy Frontier Research Center funded by the U.S. Department of Energy, Office of Science, Basic Energy Sciences.

## REFERENCES

- (1) Bard, A. J.; Faulkner, L. R. *Electrochemical Methods: Fundamentals and Applications*, 2nd ed.; Wiley: New York, 2001.
- (2) (a) Savéant, J.-M. *Chem. Rev.* **2008**, *108*, 2348. (b) DuBois, D. L. *Inorg. Chem.* **2014**, *53*, 3935. (c) Helm, M. L.; Stewart, M. P.; Bullock, R. M.; Rakowski DuBois, M.; DuBois, D. L. *Science* **2011**, *333*, 863. (d) Sampson, M. D.; Nguyen, A. D.; Grice, K. A.; Moore, C. E.; Rheingold, A. L.; Kubiak, C. P. *J. Am. Chem. Soc.* **2014**, *136*, 5460. (e) Tamaki, Y.; Vannucci, A. K.; Dares, C. J.; Binstead, R. A.; Meyer, T. J. *J. Am. Chem. Soc.* **2014**, *136*, 6854. (f) McCrory, C. L.; Uyeda, C.; Peters, J. C. *J. Am. Chem. Soc.* **2012**, *134*, 3164. (g) Valdez, C. N.; Dempsey, J. L.; Brunschwig, B. S.; Winkler, J. R.; Gray, H. B. *Proc. Natl. Acad. Sci. U.S.A.* **2012**, *109*, 15589.
- (3) (a) Costentin, C.; Drouet, S.; Robert, M.; Savéant, J.-M. *J. Am. Chem. Soc.* **2012**, *134*, 11235. (b) Costentin, C.; Drouet, S.; Robert, M.; Savéant, J.-M. *Science* **2012**, *338*, 90. (c) Costentin, C.; Drouet, S.; Passard, G.; Robert, M.; Savéant, J.-M. *J. Am. Chem. Soc.* **2013**, *135*, 9023.
- (4) Winter, M.; Brodd, R. J. *Chem. Rev.* **2004**, *104*, 4245.
- (5) Collman, J. P.; Boulatov, R.; Sunderland, C. J.; Fu, L. *Chem. Rev.* **2004**, *104*, 561.
- (6) Jasinski, R. *Nature* **1964**, *201*, 1212.
- (7) Kim, E.; Chufán, E. E.; Kamaraj, K.; Karlin, K. D. *Chem. Rev.* **2004**, *104*, 1077.
- (8) Forshey, P. A.; Kuwana, T. *Inorg. Chem.* **1983**, *22*, 699.
- (9) (a) Carver, C. T.; Matson, B. D.; Mayer, J. M. *J. Am. Chem. Soc.* **2012**, *134*, 5444. (b) Matson, B. D.; Carver, C. T.; Von Ruden, A.; Yang, J. Y.; Raugei, S.; Mayer, J. M. *Chem. Commun.* **2012**, *48*, 11100.
- (10) Lexa, D.; Rentien, P.; Savéant, J.-M.; Xu, F. *J. Electroanal. Chem.* **1985**, *191*, 253.
- (11) (a) Costentin, C.; Savéant, J.-M. *ChemElectroChem* **2014**, *1*, 1226. (b) Bernatis, P. R.; Miedaner, A.; Haltiwanger, C.; DuBois, D. L. *Organometallics* **1994**, *13*, 4835.
- (12) James, H. J.; Broman, R. F. *Anal. Chim. Acta* **1969**, *48*, 411.
- (13) Su, B.; Hatay, I.; Ge, P. Y.; Mendez, M.; Corminboeuf, C.; Samec, Z.; Ersoz, M.; Girault, H. H. *Chem. Commun.* **2010**, *46*, 2918.
- (14) See ref 1, Chapter 9.
- (15) (a) Brode, J. *J. Phys. Chem.* **1901**, *37*, 257. (b) Patrick, W. A.; Wagner, H. B. *Anal. Chem.* **1949**, *21*, 1279.